We are IntechOpen, the world's leading publisher of Open Access books
Built by scientists, for scientists

6,900
Open access books available

185,000
International authors and editors

200M
Downloads

154
Countries delivered to

Our authors are among the

TOP 1%
most cited scientists

12.2%
Contributors from top 500 universities

BOOK CITATION INDEX
CLARIVATE ANALYTICS
INDEXED

WEB OF SCIENCE™

Selection of our books indexed in the Book Citation Index
in Web of Science™ Core Collection (BKCI)

Interested in publishing with us?
Contact book.department@intechopen.com

Kinetic Features of Synthesis of Epoxy Nanocomposites

Vadim Irzhak

Abstract

Kinetic features of the formation of epoxy nanocomposites with carbon (nanotubes, graphene, and graphite), metal-containing, and aluminosilicate (montmorillonite and halloysite) fillers are considered. In contrast to linear polymers, epoxy nanocomposites are obtained only via the curing of epoxy oligomers in the presence of filler or the corresponding precursor. These additives may affect the kinetics of the process and the properties of the resulting matrix. A high reactivity of epoxy groups and a thermodynamic miscibility of epoxy oligomers with many substances make it possible to use diverse curing agents and to accomplish curing reactions under various technological conditions. The mutual effect of both a matrix and nanoparticles on the kinetics of the composite formation is discussed.

Keywords: polymer nanocomposites, epoxy matrices, nanoparticles, synthesis of composites, epoxy oligomers

1. Introduction

Since around the mid-1990s, polymer nanocomposites have become the subject of considerable attention, as evidenced by monographs, and a great number of reviews [1]. The application of nanocomposites is associated with their unique properties related to a huge specific surface and high surface energy of nanoparticles. Nanosized particles, as opposed to microinclusions and coarser inclusions, are not stress concentrators, and this circumstance facilitates a marked improvement in the mechanical properties of nanocomposites. Compared with the respective polymers, the transparency of nanocomposites does not decrease, because nanoparticles do not scatter light because of their small sizes. Depending on the type of nanoparticles introduced in polymeric materials even at a low concentration, nanocomposites acquire remarkable chemical (primarily catalytic), electrophysical, and biomedical properties, thereby opening wide potential for their use [1].

Among polymer nanocomposites, it would appear that composites based on an epoxy matrix occupy an insignificant place—nearly 10% as to the number of publications—but an ever-increasing number of papers appear annually. Moreover, the interest in them grows almost exponentially, as evidenced by the number of citations [2].

Epoxy polymers in terms of a set of properties stand out among other polymeric materials and play an important role in aerospace, automotive, shipbuilding, and other industries. Their wide application in engineering is associated, firstly, with a high processability of epoxy resins and, secondly, with the unique combination of performance characteristics of their curing products [3–5].

A high reactivity of epoxy groups and a thermodynamic miscibility of epoxy oligomers with many substances make it possible to use diverse curing agents and to accomplish curing reactions under various technological conditions [6–8]. Of no small importance are the features of synthesis processes, such as the absence of volatile products and low level of shrinkage.
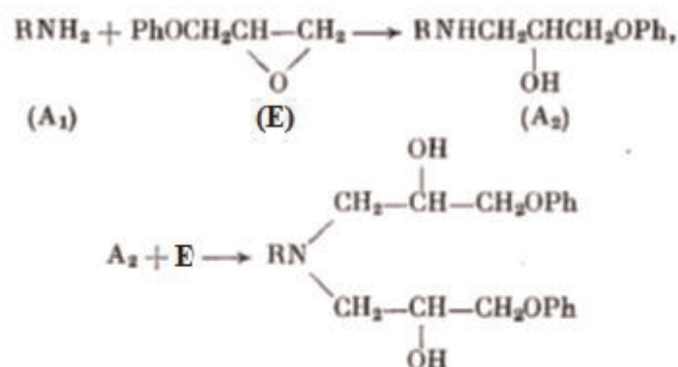
Epoxy polymers have high values of static and shock strength, hardness, and wear resistance. They possess marked thermal stability and heat resistance. Many solid surfaces form strong adhesive bonds with epoxy polymers [2, 3]. This circumstance determines their use as compounds, glues, paint and lacquer materials, and coatings, including in aerospace engineering. Epoxy nanocomposites are designed to realize the unique functional properties of nanoparticles: electric, magnetic, optical, chemical, and biological.

Information about epoxy nanocomposites is contained most completely in [2]. Reviews [9, 10] are devoted to epoxy nanocomposites with carbon nanotubes (CNTs). Some aspects of epoxy nanocomposites containing graphene were covered in [11].

Taking into consideration the urgency of the issue and the presence of recent studies not covered in the mentioned reviews, author took a chance to consider epoxy nanocomposites containing metal and mineral nanoparticles, graphene, and CNTs and to discuss kinetic features of the processes of their formation.

2. Feature of synthesis of epoxy nanocomposites

The generally accepted scheme of the amino-epoxy cure involves two main reactions of the glycidyl ether:

$$RNH_2 + PhOCH_2CH\!\!-\!\!CH_2 \longrightarrow RNHCH_2CHCH_2OPh,$$

$$\text{(A}_1) \qquad \text{(E)} \qquad \text{(A}_2)$$

$$A_2 + E \longrightarrow RN$$

Epoxy-amine cure reactions scheme.

In principle, a reaction of esterification is possible—the resulting hydroxyls with epoxy groups.

The ratio of the rate constant of the secondary amine in addition to the corresponding constant of the primary one depends on electron-donating properties of an amine and may vary with temperature. Normally this ratio varies within 0.1–0.6. It is because of accumulation of hydroxyl groups during the reaction that the process of curing epoxy oligomers under the action of amines has autocatalytic character. Kinetics is often analyzed using empirical Eq. (1):

$$\frac{d\alpha}{dt} = (k_1 + k_2\alpha^m)(1 - \alpha)^n \tag{1}$$

$$\frac{d\alpha}{dt} = (k_1 + k_2\alpha)(1 - \alpha)^n \tag{2}$$

where α is the degree of conversion of epoxy groups; the sum of exponents $m + n$ defines the overall reaction order, which is usually two. Sometimes it is assumed

that $m = 1$ (Eq. (2)). Constants k_1 and k_2 reflect the autocatalytic character of the process.

From the standpoint of formation of epoxy nanocomposites, there are two types of fillers: fillers belonging to the first type are chemically unchanged and should be reduced to the desired size in one way or another. An example is provided by CNTs, diverse minerals, and graphene. Compounds whose chemical nature changes during composite formation belong to the second type. These are, in particular, metal salts, in which cations should be reduced to the zero-valence state.

In contrast to linear polymers, epoxy nanocomposites are obtained only via the curing of epoxy oligomers in the presence of filler or the corresponding precursor. It is evident that these additives may affect the kinetics of the process and the properties of the resulting matrix. The mechanism of curing of epoxy resins is fairly complicated, because many reactions occur simultaneously and depend on such phenomena as gelation and glass transition [6, 7]. After incorporation of nanoparticles into the epoxy resin, the process of its curing becomes even more complicated. A considerable number of papers concern the kinetics of curing of epoxy systems with various types of nanoparticles.

Most of kinetic studies are using DSC. DSC analysis has shown that etherification occurs at elevated temperatures once all the primary amines are exhausted. In this case, the data are analyzed as a rule in terms of the generalized formula:

$$\frac{d\alpha}{dt} = k(T)f(\alpha) \tag{3}$$

For nonisothermal conditions the temperature varies with time with a constant heating rate, $\beta = dT/dt$.

Isoconversional kinetic analysis has shown that the reaction rate at constant conversion depends only on the temperature. In other words,

$$E_a = -Rd \ln \left(\frac{d\alpha}{dt} \right) / dT^{-1} \tag{4}$$

where E_α is the effective activation energy at a given conversion. The energy of activation was determined by varying the rate of scanning. Multistage processes show the dependence of E_α on α, the analysis of which helps not only to reveal the complexity of the process but also to identify its kinetic scheme. So, for example, starting from Eq. (1), we get [12]

$$E_a = -(k_1 E_1 + \alpha^m k_2 E_2)/(k_1 + \alpha^m k_2) \tag{5}$$

The analysis performed in [12] showed that the calculation can be reconciled with the experiment by specifying the values of E_2 and m. Thus, we can assume that Eq. (1) adequately describes the experimental data. Namely, this approach is used to study the effect of various additives on the kinetics of epoxy nanocomposites' formation.

3. Influence of the fillers on the nanocomposite synthesis process

3.1 Carbon fillers: CNTs, graphene, graphite, and carbon fiber

Taking into consideration the molecular structure of carbon nanoparticles, in particular, graphene and CNTs [13–17], it may be stated that their influence on the

kinetics of the process of curing of epoxy oligomers will be similar. Indeed, graphene, CNTs, and other compounds with the sp^2-hybridized carbon can catalyze diverse organic reactions [18–20]. Their surface energy is fairly high; therefore, the adsorption of various molecules is typical of them [21–24]. The components of epoxy binders are not exceptional in this respect. Adsorbed molecules may be involved in the process of matrix formation in a certain manner.

In work [25] the high-temperature isothermal curing of tetraglycidyl-4,4′-diamino-diphenylmethane with 4,4′-diaminodiphenyl sulfone (DDS) in the presence of multi-wall CNTs was investigated.

The typical technique used to prepare the reaction mixture for kinetic studies of the process will be described below, and the techniques described in other papers may differ from the typical one only in some details.

A mixture of an epoxy resin with preliminarily purified multi-wall CNTs was sonicated for 2 h and placed in an oil bath at temperature of 120°C, and the stoichiometric amount of a curing agent was slowly added under continuous mechanical stirring until formation of a homogeneous mixture. This process took nearly 10 min.

The kinetics was analyzed using Eq. (1). It was found that with the increase in concentration of CNTs, constant k_1, which defines the initial rate of reaction, grows, while the corresponding activation energy drops. The autocatalytic constant k_2 is practically unaffected by the presence of tubes. Xie et al. [25] believe that these effects may be attributed to the catalytic effect of surface hydroxyl groups that arise as a result of oxidation during the purification of CNTs.

The initial acceleration of the reaction under the action of single-wall CNTs was also observed [26], but the magnitude of this effect was insignificant. At the same time, the glass-transition temperature T_g decreased, thus suggesting a reduction in the degree of cross-linking of the matrix [6].

The effect of concentration and type of CNTs (single-, double-, and multi-wall) on the kinetics of reaction between low-viscosity mixture of epoxy oligomers and amine curing agents was studied by Esmizadeh et al. [27]. The analysis was conducted in terms of the equation:

$$\frac{d\alpha}{dt} = k(T)\alpha^m(1 - \alpha)^n \qquad (6)$$

It was shown that the type of CNTs exerts almost no effect on kinetic parameters possibly because of their low concentration (0.01%). At a concentration of 0.1, 0.2, and 0.5%, the rate constant changes nonmonotonically, but on the whole it is lower than that in the absence of CNTs. The energy of activation increases from ~6 to ~9 kJ/mol. The heat of reaction decreases, indicating the incompletion of the process. This is also evidenced by a decrease in the high-elasticity modulus, i.e., matrix network density. In accordance with [27], the observed effects may be explained by the increase in the viscosity and thermal conductivity of the system in the presence of CNTs, although these properties were not estimated.

Multi-wall CNTs, when taken at low concentrations (0.5%), slightly accelerate the reaction of amine curing of bisphenol F diglycidyl ether, while at higher con-centrations (1.5%) decelerate this reaction as shown by Visco et al. [28]. They believe that the rate of the process is controlled by viscosity of the system.

The curing of an epoxy resin is regarded as a heterogeneous phase formation process, and the role of multi-wall CNTs is discussed from this viewpoint by Susin et al. [29]. They believe that the tubes restrict the local free volume and assist in the development of the heterogeneous morphology in resin, especially at high content of multi-wall CNTs. At the same time, with the increase in their concentration

(to 1%), the ultimate heat of reaction increases, while the energy of activation decreases.

Most of kinetic studies are aimed at gaining insight into the effect of functionalized CNTs using DSC. Rahaman and Mohanty [30] presented the data of the influence of multi-wall CNTs carrying COOH groups on the process of curing of epoxy resin EPOLAM with anhydride of 1,2,3,6-tetrahydroxymethyl-1,3,6-methanephthalic acid. According to these authors, this dependence provides evidence that in the presence of multi-wall CNTs, the degree of cross-linking increases; as a result, the mobility of unreacted groups declines. The closeness of the curves at the beginning of the curing process indicates that the addition of CNTs does not affect the value of E_1. From the form of the divergence of the curves in the course of the reaction, it follows that the entrainment of the filler leads to an increase in E_2.

Note that methods using the dependence of a change in the exothermal peak on the rate of heating cannot provide reasonable isothermal predictions for the kinetics of curing of epoxy compounds because of the autocatalytic character of the process [6, 7]. The presence of at least two kinetic constants, as in Eq. (1), should be taken into account.

In this context, deserve attention other methods, which, depending on the type of study or the nature of epoxy resins, can be successfully used [31]. Among them, for example, the method of luminescence spectroscopy makes it possible to determine the degree of conversion with high accuracy at the final stage of reaction. This is hardly achievable by other methods. Analysis with the aid of a rheometer provides information about the time of gelation which cannot be obtained by another method.

The DSC studies [32] showed that multi-wall CNT with COOH functionalization act as catalysts, stimulating the initial stage of curing of bisphenol A diglycidyl ether (BADGE). This accelerating effect is noticeable even at a 1% content of multi-wall CNTs. Nonfunctionalized multi-wall CNTs decrease the degree of cross-linking, as evidenced by a lower overall heat of reaction and lower glass-transition temperatures of the nanocomposites compared with the neat epoxy resin. At the same time, the functionalization of multi-wall CNTs increases the degree of cross-linking.

Compared with the neat epoxy resin, 1% of carboxylated multi-wall CNTs decreases the heat of reaction and increases the energy of activation [33]. Fluorinated tubes insignificantly influence the value of E_a but lower the ultimate degree of conversion Q_{lim}.

The grafting of butylamine onto plasma- and CF_4-treated single-wall CNTs markedly improves the ultimate conversion, whereas clean tubes, when the reaction is accomplished in the nonisothermal regime, have no effect on this parameter, while in the case of the isothermal regime (30°C), they decrease it [34].

There was another conclusion [35] that clean and aminated single-wall CNTs reduce the ultimate heat of reaction. Tubes with the grafted epoxy groups give almost the same value of heat as that obtained in the curing of resin without any filler: 355 versus 362 J/g. It is possible that different results may be attributed to different concentrations of single-wall CNTs.

The kinetic analysis of the curing process in terms of Eq. (1) does not reveal marked differences in the values of constants and exponents for the systems of interest. However, it was shown [36] that the introduction of 3% of clean multi-wall CNTs does not influence the kinetics of reaction, but tubes with grafted amino groups decrease the constant k_1 by factor of almost 2.5, increase k_2 by factor of 3, and decrease exponent m from 0.53 to 0.27.

Multi-wall CNTs with amino groups decelerate the curing of BADGE with 2-ethyl-4-methylimidazole at concentrations of 0.5 and 1 wt % [37], but the deceleration effect vanishes at a concentration of nanoparticles of 3%. However, in this

case, the value of ultimate reaction heat decreases as well. Note that clean multi-wall CNTs accelerate curing of the same reaction system [32].

The impact of multi-wall CNTs carrying acidic and amino groups on the process of curing was studied by Raman and luminescence spectroscopy [38]. Throughout the reaction conducted in the presence of nanoparticles, the rates were higher than the neat resin. The difference in the rates of curing was explained by homogeneity of the sample and the presence of chemical groups.

The kinetics of the amine curing of BADGE in the presence of multi-wall CNTs functionalized by oxygen-containing groups using viscometry and transmission electron microscopy along with calorimetry was analyzed [39]. The samples of multi-wall CNTs had different values of specific surface S. This factor was found to be decisive in the kinetic study of reaction: if at the onset the rates were equal, then, by the time of attaining the maximum rate W_{max}, the higher the value of S, the more pronounced the deceleration of the process, so that the time of attaining W_{max} increased. Afterward, the inverse effect was observed, namely, acceleration, so that the higher the value of S, the more pronounced the final heat release. The rheokinetic study demonstrated that the time of a sharp gain in viscosity of the system (the gel point) also shifts to longer times with an increase in S. However, variation in the concentration of multi-wall CNTs (to 5%) insignificantly influences the kinetics of reaction.

The kinetic features of the process may become understandable if the micrograph of the epoxy composition which is measured at the initial stage of curing performed in the presence of multi-wall CNTs is examined (**Figure 1**). It is seen that compact polymer structures grow along the tube. Evidently, hydroxyl groups grafted on the surface catalyze the reaction of epoxy groups with amine [7] to give rise to new hydroxyl groups accelerating this reaction. In doing so, the process of polymer formation is localized, and the reaction assumes the frontal character. The natural consequence of the localization process is the formation of ineffective cross-links. Therefore, the value of critical conversion increases, and correlation is observed between the time of a sharp gain in viscosity and the specific surface of multi-wall CNTs.

It was shown that graphene oxide (GO) accelerates the curing of tetraglycidyl-4,4′-diaminodiphenylmethane with 4,4′-diaminodiphenyl sulfone [40]. According to this work, this effect is related to the presence of hydroxyl and carboxyl groups on the surface of GO.

The kinetics of the nonisothermal curing of BADGE with liquid poly(amido-amine) in the presence of amine-functionalized GO using Eq. (6) was investigated [41]. It is seen that for the systems without any filler and in the presence of GO containing NH_2 groups, the parameters of this equation are similar. At the same time, GO slightly decelerates the process.

The mixture of BADGE and 1,1,2,2-tetra(p-hydroxyphenyl)ethane tetraglycidyl ether with diethyltoluenediamine in the presence of graphene was cured [42]. It was shown that the latter somewhat accelerates the reaction and increases T_g by 15–25°C. Previously, the same authors showed using Eq. (1) that this effect is
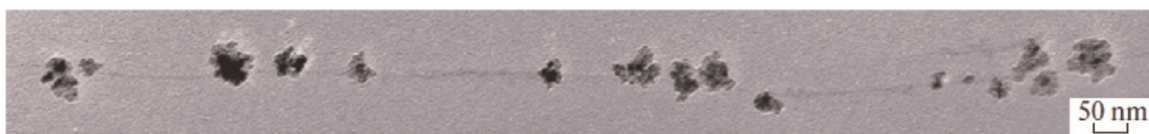

Figure 1.
Initial stage of curing of the epoxy matrix in the presence of COOH-functionalized CNTs. Reprinted with permission from IAPC "Nauka" [39].

associated with an increase in constant k_1 and the functionalization of graphene by amine enhances the effect of the filler [43].

The IR spectral analysis of the curing of BADGE with 4,4'-diaminodiphenylmethane in the presence of GO permitted to obtain kinetic curves for both epoxy groups and primary, secondary, and tertiary amino groups [44]. These studies made a considerable contribution to gaining insight into the mechanism of reaction. It was shown that the original GO has no effect on the overall kinetics of the process and even decelerates the consumption of primary amino groups. But after autoclave purification, GO increases the rate of reaction of epoxy groups by more than factor of 2 and the rate of reaction of primary amino groups by factor of 1.8. As was shown by X-ray photoelectron spectroscopy, purification leads to a marked reduction in the amount of oxygen-containing groups on the surface of GO. The glass-transition temperature of a nanocomposite based on the crude GO is much lower than that of the epoxy matrix, whereas the purification of GO causes an increase in this parameter, although T_g does not attain the T_g value of the matrix.

The influence of various graphite fillers (graphite with a high surface area, graphite oxide, and exfoliated graphite oxide) on the reaction of epoxy ring opening of BADGE by amines—primary (benzylamine and cyclohexylamine) and secondary (dibenzylamine)—and hydroxyl (benzyl alcohol) was studied [45]. These data indicate the strong catalytic effect of fillers on the reaction with amines. This effect is the most pronounced for the exfoliated graphite oxide. In the case of benzyl alcohol, interaction with epoxy groups was observed only for graphite oxide. A similar effect was caused by fillers on the process of matrix formation: in the presence of graphite fillers, the rate and heat effect of the reaction grow, and the gel point shifts to smaller times.

In essence, analogous data were reported by Mauro et al. [46]. These authors believe that a marked rise in the T_g of nanocomposites compared with the neat matrix is an evidence of the catalytic effect of graphite with a high surface area (308 m^2/g) and graphite oxide. The catalytic effect of graphite was confirmed using the reaction of epoxystyrene with benzylamine.

On the other hand, it was found that the samples of graphite oxide with carboxyl or amino groups have almost no effect on the kinetics of nonisothermal curing of BADGE with 4,4'-diaminodiphenylmethane [47]. Possibly, this is related to a low concentration of the fillers (0.5%).

The effect of carbon nanofibers (diameter of 100–200 nm and length of 30–100 μm) oxidized in a solution of nitric acid and then treated with 3-glycidoxypropyltrimethoxysilane on the kinetics of curing of epoxy resin Cycom 977 described by Eq. (1) was studied [48]. It was shown that all kinds of fibers exert a catalytic effect which manifests itself as an increase in ultimate conversion and growth of kinetic constants k_1 and k_2. Note that E_{a1} decreases, while E_{a2} increases. In terms of catalytic efficiency growth, the fibers may be arranged in the following sequence: untreated, oxidized (COOH groups on the surface), and treated with silane (epoxy groups on the surface).

The catalytic effect of a carbon nanofiber was observed: the ultimate conversion and the kinetic constants in Eq. (1) increase, while the respective activation energies decrease [49]. The higher activity is exhibited by fiber whose surface is modified through the oxidative polymerization of aniline (in accordance with the authors, the "nanograssy" coating).

The above results are rather contradictory, which is probably caused by ambiguity in the concentration of the filler, uncertainty in the degree of dispersion, and the magnitude and structure of its surface.

3.2 Noncarbon fillers: oxides of metals and silicon

The effect of Al_2O_3 nanoparticles on the kinetics of polycondensation of BADGE under the action of diethylenetriamine using modulated DSC was explored [50]. As a result, not only the rate of the process was registered, but also variation in the heat capacity of the system during the process was monitored. It was shown that the filler increases the rate of reaction but decreases the ultimate heat. Viscosity measurements confirmed that the formation of the polymer network accelerates in the presence of nanoparticles, and the gel point shifts not only with time but also with conversion. This implies that nanoparticles are directly involved in the formation of intermolecular bonds. At the same time, experiments with water additives revealed that nanoparticles affect the kinetics of the curing reaction in qualitatively the same manner as Al_2O_3 nanoparticle [51]. The authors inferred that water adsorbed by nanoparticles is responsible for the catalytic effect.

DSC was used to examine the effect of additives of Al_2O_3 and ZnO nanoparticles on the curing of BADGE with o-tolylbiguanidine [52]. Both oxides decelerate the reaction but increase the ultimate limiting degree of conversion. Exponents m and n in Eq. (6) remain almost unchanged, whereas the activation energy decreases. Note that in the case of ZnO, this decrease is considerable.

At a fairly low concentration (1 and 5%), ZnO nanoparticles accelerate the reaction of BADGE with 2,2'-diamino-1,1'-binaphthyl; at concentration of 10%, their catalytic efficiency declines, while at content of 15%, retardation is observed [53]. Compared with the neat matrix, nanocomposites feature higher values of ultimate heat and glass-transition temperature with the maximum values corresponding to 5% content of nanoparticles. Probably, reduction in the catalytic activity of nanoparticles with increasing concentration may be attributed to their aggregation; as a result, the effective surface decreases.

Ghaffari et al. [54] studied how the size of ZnO nanoparticles affects the kinetics of BADGE curing with poly(aminoamide). Nanoparticles were sheets with a thickness of nearly 20–40 nm, while microparticles were rods with a length of $\sim$1 μm. Analysis was performed using Eq. (5). It was found that the autocatalysis of reaction is absent; that is, $m = 0$ and n is somewhat above unity. For both composites, compared with the neat matrix, the energy of activation decreases, but the rate constant slightly grows in the case of the microcomposite and declines in the case of the nanocomposite.

BADGE with the propylenimine dendrimer carrying eight end groups -NH_2 in the presence of Fe_2O_3 nanoparticles was cured [55]. The latter manifested the catalytic effect. The higher the concentration of nanoparticles, the more pronounced the increase in ultimate conversion and glass-transition temperature. It is shown that the kinetics of formation of the nanocomposite containing 10% Fe_2O_3 is adequately described by Eq. (2). No data are available for other systems, including the neat matrix. A similar result was reported in [56]. It was shown that the kinetics of curing of glycerol diglycidyl ether with 3,3'-dimethylglutaric anhydride in the presence of Al_2O_3 obeys Eq. (2).

Nanoparticles of metal oxides are able to adsorb components of the reaction system to one extent or another [57]. Possibly, their kinetic role is associated with this property.

Direct measurements of the complex specific heat capacity demonstrated that the interaction of SiO_2 nanoparticles and BADGE molecules is very weak [58]. At all stages of polymer network formation, the interaction of nanoparticles and matrix is of a physical origin. The effect of the filler on the kinetics of curing was insignificant.

In contrast, acceleration of the process was observed [59, 60]. The kinetic studies revealed that the catalytic effect of SiO_2 nanoparticles is related to the presence

of hydroxyl groups on their surface [61]. When the latter groups are changed for epoxy groups, the effect of nanoparticles on the kinetics of BADGE reaction with *m*-phenylenediamine is eliminated.

3.3 Minerals

For polymer nanocomposites, the most popular fillers from the class of minerals are layered silicates [62], which are sometimes called nanoclays, in particular, montmorillonite (MMT). The structure of its crystal lattice is such that it can adsorb various ions (mostly cations) and swell in polar liquids owing to their penetration into the interlayer space [63, 64].

At the nanometer scale, MMT is composed of three-layer stacks ∼0.7 nm in thickness and several hundred nanometers in length and width. At micron level, these stacks are united into primary particles with interlayer distance of about 1.35 nm. At higher level, they form aggregates. During formation of nanocomposites, stacks should be exfoliated in order to reach a high area of contact with the matrix. In order to facilitate exfoliation, the surface of stacks should be treated for the purpose of changing their hydrophilic nature to hydrophobic, because the hydrophilic character of the silicate surface hampers the dispersion of MMT. Neutral organic compounds may form complexes with interlayer cations; for example, alkylamines are transformed into alkylammonium cations. These properties of MMT govern the kinetic features of formation of epoxy nanocomposites.

In the absence of the curing agent (1,3-phenylenediamine), the modified MMT and even the unmodified MMT promote the homopolymerization of BADGE at a high temperature [65]. Depending on the nature of the intercalated modifier (octadecyl-, trimethylstearyl-, methyldihydroxyethylammonium), MMT may either catalyze the reaction of the epoxy oligomer or react with a prepolymer or a curing agent.

At the same time, it was found that MMTs modified with alkylamines weakly accelerate [66–68], retard [69], or do not affect at all [70] the kinetics of curing of epoxy oligomers with amines. A weak acceleration was also observed for the unmodified MMT and MMT with intercalated 3-aminopropylethoxysilane [71].

Thus, it should be stated that the rate of curing of epoxy oligomers is almost insensitive to the presence of MMT. However, the kinetics of formation of polymers is not reduced only to a change in the concentration of reactants: structure formation should be taken into account. Even to a higher extent, this applies to a nanocomposite, whose properties are determined not only by structural levels of polymer matrix but also by the structure of nanoparticles and the character of their distribution in the material bulk.

As was noted above, MMT requires exfoliation. Namely, this process occurs during the chemical reaction, and its efficiency depends on the reaction conditions. For example, it was shown [72] that the cationic polymerization of triglycidyl-*p*-aminophenol occurs within the interlayer space, which entails the exfoliation of MMT, whereas with DDS the epoxy oligomer reacts outside the interlayer cavity. An increase in temperature is favorable for the former reaction: ultimate conversions inside and outside the cavity are 0.19 and 0.74, respectively, at 120°C or 0.76 and 0.77 at 180°C.

The optimum structure of epoxy composites was achieved when BADGE was cured with poly(ester diamine) in the nonisothermal regime at low rise in temperature (2.5 and 5 K/min) [73]. Small-angle X-ray scattering studies revealed the exfoliation of MMT in the matrix. The authors of [74] used hyperbranched polyethylenimine with end amino groups as a curing agent and attained effective exfoliation. A comparison of three systems, such as

triglycidyl-*p*-aminophenol + DDS, BADGE + poly(ester diamine), and BADGE + hyperbranched polyethylenimine, showed [75] that the exfoliation ability of MMT decreases in the mentioned sequence.

As was reported in [76], the nonisothermal curing of epoxy oligomers with amines in the presence of MMT includes four different reactions: formation of the matrix via the interaction of epoxy groups with the diamine curing agent, intracavity homopolymerization, and two homopolymerization reactions outside MMT which are catalyzed by onium ions of organically modified clay and tertiary amines.

X-ray diffraction was used to probe the exfoliation of MMT intercalated by octadecylammonium during the isothermal curing of BADGE with DDS [77]. It was shown that this process may be divided into three different stages (**Figure 2**).

The first stage is related to the penetration of BADGE into the interlayer space of MMT; at the second stage, the cationic polymerization of the epoxy resin catalyzed by ammonium takes place; and at the third stage, BADGE sorbed by MMT is cured with amine.

In order to identify the intracavity polymerization, mixture of MMT and triglycidyl-*p*-aminophenol was held at various temperatures for tens of days in the absence of the amine curing agent. Afterward, DDS was added and the curing process was conducted in the nonisothermal regime [78]. A similar procedure was employed for the system BADGE-MMT-poly(ester diamine) [79]. At the first stage, the epoxy equivalent and the glass-transition temperature increased. This technology makes it possible to improve both the degree of dispersion of MMT in the epoxy resin and the subsequent exfoliation of the clay during formation of epoxy nanocomposites. The period of the intracavity polymerization was reduced to tens of minutes by the use of complex $BF_3 \cdot C_2H_5NH_2$ as a catalyst [80].

An attempt to accomplish the intracavity polycondensation was made by Jagtap et al. [81]. In contrast to the commonly used MMT modifiers, i.e., polyalkylamines, they used half-neutralized salt of poly(ester diamine), which was intercalated via ionic exchange in an aqueous-organic solution, assuming that these macromolecules, when fixed by the ionic end on the walls of the cavity, will react with epoxy groups of the binder via its free amine end. However, no direct evidence for this reaction is available [81].
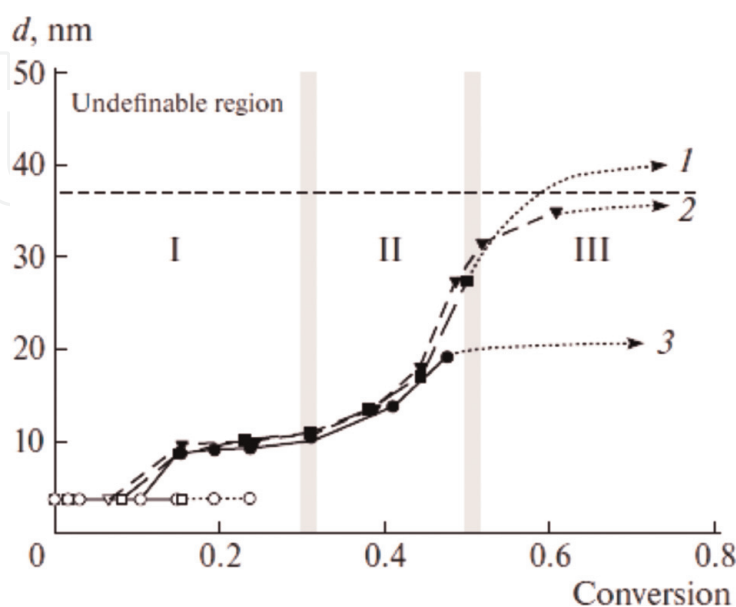

Figure 2.
Change in distance d between MMT sheets during the isothermal curing of BADGE at (1) 140, (2) 130, and (3) 120°C. Roman numerals denote stages of the exfoliation process. Arrows indicate the expected tendency of exfoliation. Reprinted with permission from Am. Chem. Soc. [77].

3.4 Metal-containing nanoparticles synthesized in situ

The synthesis of metal-containing nanoparticles for producing nanocomposites may be accomplished by various physical processes on the preformed matrix containing molecules of appropriate precursors [82–87]. Physical methods of obtaining metal-containing nanoparticles (photolysis, radiolysis, and thermolysis) are as a rule accompanied by chemical reactions leading to their formation. An important factor is the diffusion of preformed substances (metal atoms): the glassy state of the matrix provides a considerable obstacle to diffusion. For example, *N*-cetylpyridinium tetrachloroaurate was dissolved in methyl methacrylate and, after polymerization of the latter, was subjected to UV radiation. However, the formation of gold nanoparticles was registered only at temperatures above T_g of the polymer [88].

A substantially different method involves the combination of processes of formation of matrix and metal-containing nanoparticles, i.e., formation of nanocomposites in situ.

The main chemical method used at moderate temperatures includes the reduction of chemically bound metal atoms in nonpolar media. These methods of chemical reduction are the subject of most publications [83, 87, 89–93]. Mechanisms controlling formation of metal-containing nanoparticles in situ are highlighted in the review [94].

The transformation of the resulting single-valence atoms, or monomers, into nanoparticles includes nucleation stages with formation of primary clusters or stable particles, their growth by addition of monomers, possible subsequent coagulation, and/or Ostwald ripening. The kinetics of all these stages determines the size distribution function which strongly affects the ways and possibilities of the nanoparticles and corresponding nanocomposites' application. An important role in this is played by a polymer medium in which chemical reactions take place, including the ability of its components or fragments of macromolecules to be adsorbed on the particles, as well as the possibility of formation of micelle-type structures.

With rapid decay of the precursor, there will be a supersaturation of the system with a monomer. In this case, in the first approximation, nucleation will be described by Gibbs-Volmer-Frenkel thermodynamic theory [95, 96], according to which the radius of the critical nucleus is determined by the formula:

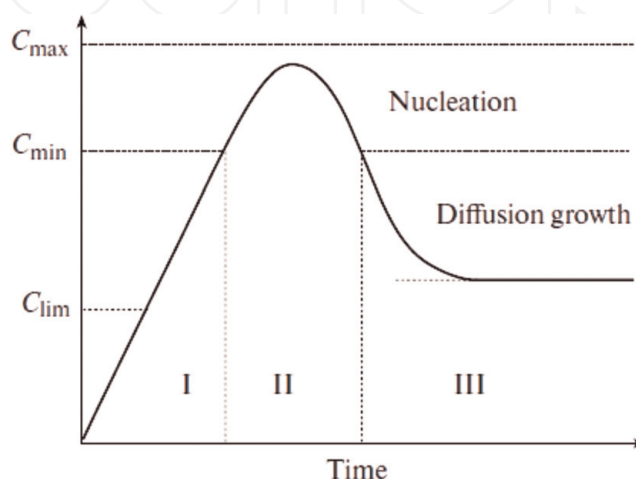$$r_c = \frac{2\sigma V_m}{RT \ln S} \qquad (7)$$

Figure 3.
LaMer pattern (see text for explanations).

where r_c, σ, and V_m are radius, surface tension, and molar volume of the critical nucleus, R is the gas constant, T is temperature, and S is the supersaturation. In this case, the nucleus will be unstable if $r < r_c$, and it stabilizes when $r \geq r_c$.

A qualitative picture of nucleation kinetics on the basis of the classic thermodynamic notions was proposed by LaMer and Dinegar [97]. The pattern illustrating their idea is shown in **Figure 3**.

Rapid increase in the concentration of monomer will lead to the achievement of the critical value of C_{min} (region I, the stage of prenucleation) and then overcome C_{min}. Exceeding this value gives rise to proper nucleation. Because of the balance between the rate of formation of the monomer and its expenditure consumption on nucleation and growth of the generated nuclei, the concentration will reach a peak, C_{max}, and then begin to decrease due to an increase in consumption for growth and again reach the critical level of C_{min}, marking the end of the nucleation stage (region II). After that, the concentration of the monomer will continue to decrease to the equilibrium value of C_0, expending on the growth of nucleus without renucleation, due to the fact that the supersaturation is below the critical level (region III).

Although short spatial and temporal scales of the nucleation stage hamper the direct observation of the classic process, to trace the time-resolved formation of silver CNs using small-angle X-ray scattering in situ was managed [98]. Silver perchlorate was reduced with sodium boron hydride in an aqueous solution. As shown in **Figure 4**, the nanoparticles' nucleation kinetics corresponds to the LaMer pattern: the number of particles initially grows without any appreciable change in their sizes, attaining a maximum in fractions of a second. Further, the number of nanoparticles descends, and their radius increases. This corresponds to stage III in the pattern, and nanoparticles interact with each other alongside with their simple growth via the reaction with monomers, i.e., the aggregation mechanism is engaged.

However, under conditions of formation of composites, it is hardly possible to implement such a mechanism. An alternative variant was obtained in [99]. When studying the synthesis of gold by reducing $HAuCl_4$ with sodium citrate, it was shown that rapid nucleation is not observed; on the contrary, the kinetic curve of accumulation of critical nuclei is S-shaped with a more or less extended induction period. The authors suggested that such features of the process are due to redox reactions leading to the conversion of gold cations to a zero-valent atom and citrate ion to acetone dicarboxylic acid. In this case, the supersaturation of the system by
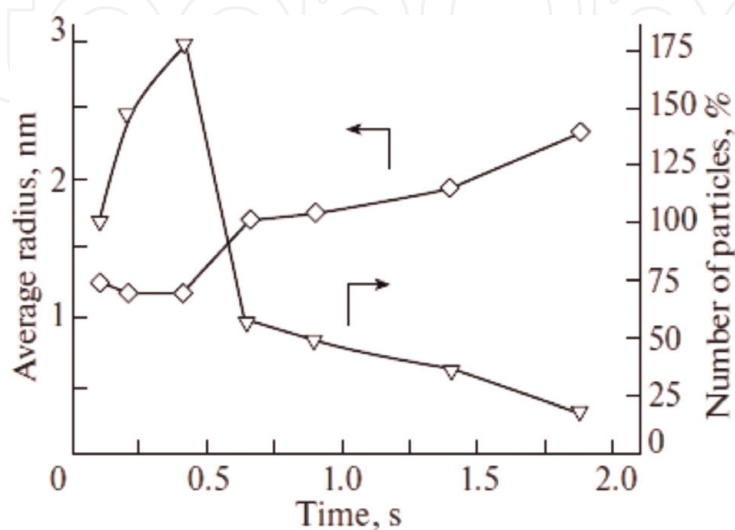

Figure 4.
Kinetics of change in the average radius and number of particles for first 2 s. Reprinted with permission from Am. Chem. Soc. [98].

the monomer, Au(0), is absent. Obviously, in this case the concept of a critical nucleus becomes meaningless.

Later it was established that S-shaped kinetics is inherent in many metals with variable valence (see, e.g., the review [100]). To describe such processes, a rather simple two-step scheme was proposed by Watzky and Finke [101]:

$$A \xrightarrow{k_1} B$$
$$A + B \xrightarrow{k_2} B_2$$

(8)

The first stage is the slow nucleation of "kinetically efficient" clusters B from precursor A, and the second stage is the particle's fast growth reaction. In the original studies, in particular in [99], A represented complex $[(n\text{-}C_4H_9)_4N]_5Na_3[(1,5\text{-}cyclooctadiene)Ir\,P_2W_{15}Nb_3O_{62}]$, and B was the catalytic surface of a $Ir_n(0)$ nanocluster.

Studies of a wide range of systems show (see [94]) that the value depends on the number of catalytic active nuclei, namely, their ratio with increasing ratios k_2A_0/k_1 for practically unchanged diameters of the order of 2 nm. These factors—the medium, active additives, and temperature—make it possible to achieve the formation of an almost monodisperse distribution (width not exceeding 15%) of the nanoparticles with a size determined, as a rule, by a "magic number" (number of atoms in the outer filled nanoparticle shell: 13, 55, 147, 309, etc.).

The processes of formation of zero-valence atoms or other monomers inevitably lead to their clustering. To stabilize clusters in a nonpolar solution, it is necessary to have amphiphilic molecules capable of forming adsorption layers and thereby form inverse micelles from the nanoparticles.

At the same time, when the epoxy nanocomposite films are stored under light for a while, the optical density $D_{\max}$ in the region of the surface plasmon resonance of silver nanoparticles decreases. Similar changes are observed in the spectra and at storage of films in the dark [102] (**Figure 5**). The kinetic curves are described by the first-order equation (**Figure 5a**, straightening in **Figure 5b**)

$$D_{\max} = D_{\lim} + A \exp\left\{-kt\right\}$$

(9)

in which $D_{\lim}$ = 0.534 (in the dark) and 0.42 (in the light).

Accordingly, the value of the limiting conversion of nanoparticles under light is higher than in dark: the conversion under light is 0.29, while in dark, the conversion is 0.11.

The decrease in $D_{\max}$ in time means a drop in the total concentration of metallic silver, apparently due to its "dissolution." The relatively recent discovery of digestive ripening (DR), which represents the transfer of atoms from large metal nanoparticles to smaller ones [94, 103], indicates the possibility of such a process.

Although the mechanism of the DR process is not fully understood, there are grounds to believe that the equation proposed in [104, 105] for describing the kinetics of Ostwald ripening (OR) is applicable to DR. The latter is one of the options for the growth of the nanoparticles, when large particles grow at the expense of small particles. According to the theory, the change in the radius r of a spherical particle in time will obey the equation:

$$\frac{dr}{dt} = \frac{K_D}{r^2}\left(\frac{r}{r_c} - 1\right)$$

(10)

where $K_D = \frac{2\sigma V^2 DC_0}{RT}$, D is diffusion coefficient, V is molar volume, and C_0 is solubility of the monomer; R is the gas constant and T is temperature; r_c is determined by equation (7).
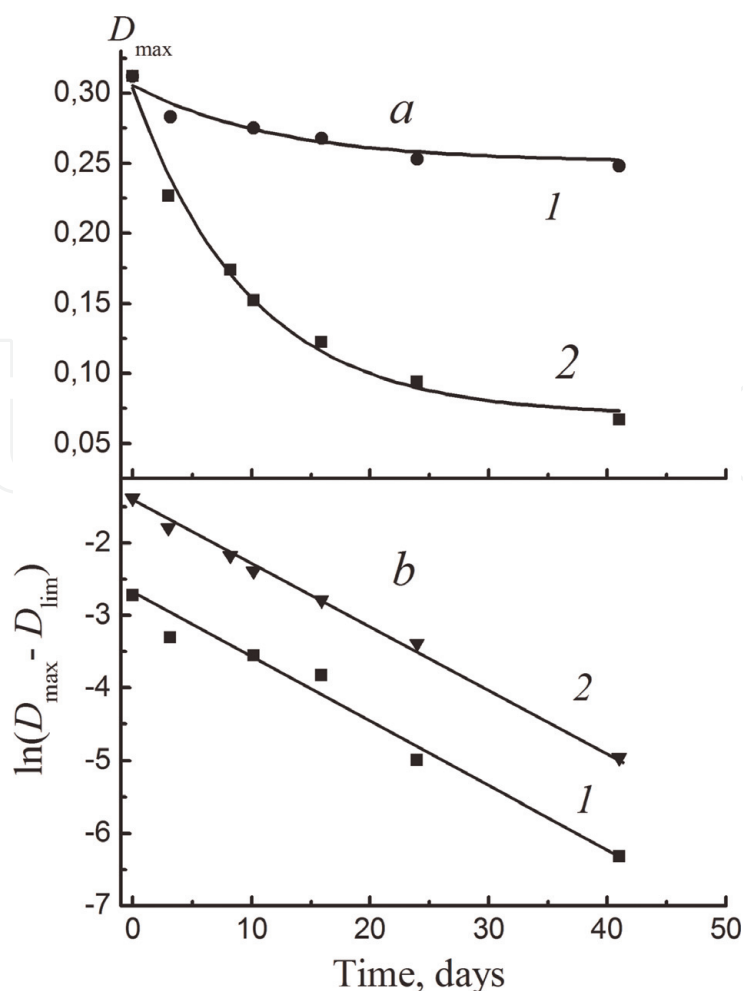
Figure 5.
Kinetics of the decrease in the concentration of silver nanoparticles in dark (1), in light (2), in natural (a), and in semi-logarithmic (b) coordinates. Reprinted with permission from IAPC "Nauka" [102].

As can be seen, the particles grow if $r \geq r_c$, and their dimensions decrease otherwise. This is the physical meaning of the phenomenon of OR.

A vivid example of reversible OR and DR was demonstrated by Xin and Zheng [106]. They observed fluctuating growth of bismuth nanoparticles in the absence of precursor at 180°C. The reaction system consisted of a limited number of large Bi nanoparticles (80–150 nm in diameter) in a solution of oleylamine (surfactant) and dichlorobenzene. The Bi nanoparticles served as a source of monomeric Bi(0).

The process includes formation and growth of small particles due to large ones (DR) with simultaneous OR. The total number of particles increased for a while and then changed to the fluctuation mode. The total volume of content fluctuated near a certain level evidently given by the total volume of initial Bi nanoparticles. The size of each of the observed particles and their assemblies experienced similar fluctuations.

Obviously, the first stage of the DR process is the disassembly of small nanoparticles on zero-valence atoms and metal clusters. Under normal conditions, they subsequently lead to formation of nanoparticles, which require their diffusion displacement. But under the conditions of a glassy matrix, diffusion is difficult, if not forbidden at all. Therefore, the entire process is reduced to the first stage, i.e., "dissolution" of large nanoparticles with the formation of zero-valence atoms and silver clusters. The presence of a limit, apparently, is due to the saturation of the boundary zone surrounding the particle by the zero-valence atoms and clusters of silver formed.
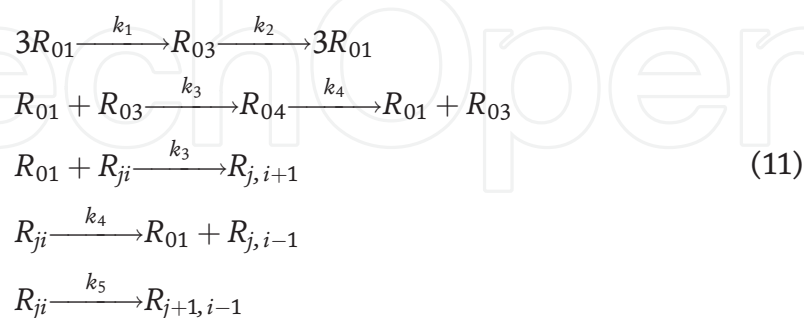
As precursors soluble in organics, complexes of univalent gold $[O(AuPR_3)_3]$ (CF_3SO_3) (R = Ph or CH_3) [107], $[RN(CH_3)_3][Au(SC_{12}H_{25})_2]$ (R = C_8H_{17}, $C_{12}H_{25}$, and $C_{14}H_{29}$), and $[(C_{18}H_{37})_2N(CH_3)_2][Au(SC_{12}H_{25})_2]$ were proposed by Nakamoto et al. [108]; salts of organic acids with a fairly bulky (even high-molecular-mass [109–111]) radical, such as silver myristate $C_{13}H_{27}COOAg$, copper oleate $(C_{18}H_{33}COO)_2Cu$, silver oleate, silver octanoate $C_7H_{15}COOAg$, silver stearate $C_{17}H_{35}COOAg$, silver 2-hexyldecanoate p-$C_8H_{17}CH(n$-$C_6H_{13})COOAg$, *cis*9-octadecanoate p-$C_8H_{17}CH=CH(CH_2)_7COOAg$, and silver neodecanoate $CH_3(CH_2)_3C(CH_3)_2COOAg$, have enjoyed popularity [107, 112–117].

However, the nonideal state of solutions of these compounds should be taken into account. This implies that, when a certain concentration is exceeded, precursors in solution are united into associates, i.e., are clustered. Evidently, this circumstance cannot be disregarded when considering feasible mechanisms governing formation of metal-containing nanoparticles.

The silver nanoparticles by the reduction of alkyl carboxylates in trimethylamine at 78°C were synthesized [118, 119]. It was found that the induction period grows and the maximum rate decreases in the following sequence: decanoate, myristate, and stearate. But in this sequence, the length of the hydrocarbon radical of carboxylates (C_9, C_{13}, and C_{17}) increases. It is reasonable to assume that solubility grows in the same sequence and, hence, the possibility of formation of clusters decreases. Thus, there is a direct relationship between the rate of formation of nanoparticles and the concentration of precursor clusters.

This idea underlies the theory of formation of metal-containing nanoparticles from precursors of the silver carboxylate type via their reduction which was put forth [120].

The model adopted for the formation of metal-containing nanoparticles may be presented as follows. Carboxylates reversibly form triangular and tetrahedral clusters. The development of larger clusters is not allowed because of steric reasons. The reduction of cation in them occurs. As a result, the adsorption of new salt molecules becomes possible. Indeed, if for carboxylates the tetrahedral structure is limiting, then the metal atom in the limit may be surrounded by 12 molecules (the icosahedron structure). It is assumed that the concentration of the reducing agent is high, so that the corresponding reaction is pseudo first order. Thus, the kinetic scheme may be written as follows:

$$3R_{01} \xrightarrow{k_1} R_{03} \xrightarrow{k_2} 3R_{01}$$
$$R_{01} + R_{03} \xrightarrow{k_3} R_{04} \xrightarrow{k_4} R_{01} + R_{03}$$
$$R_{01} + R_{ji} \xrightarrow{k_3} R_{j,\,i+1} \tag{11}$$
$$R_{ji} \xrightarrow{k_4} R_{01} + R_{j,\,i-1}$$
$$R_{ji} \xrightarrow{k_5} R_{j+1,\,i-1}$$

where (i = 0, 1, 2, …; j = 3, 4,…).

Here R_{ji} denotes clusters composed of i carboxylate molecules and j atoms of the zero-valence metal. Accordingly, R_{01} is the initial carboxylate, R_{03} is the cluster of the triangular carboxylate, and R_{04} is the cluster of the tetrahedral carboxylate. Reactions with constants k_1 and k_2 are responsible for the formation and dissociation of associates consisting of three carboxylate molecules, and reactions with constants k_3 and k_4 correspond to the addition of one molecule to cluster R_{ji} and its detachment. The reaction with constant k_5 involves reduction of the bound metal in a cluster.

A system of equations corresponding to scheme (11) was analyzed with a wide variation in kinetic constants. It was shown that the values of k_2, k_4, and k_5 have a slight effect on kinetics of the process. The decisive role is played by constants k_1 and k_3, that is, those constants that determine reactions giving rise to clusters, including mixed clusters.

The kinetics of the process is characterized by the existence of the induction period in the reaction of carboxylate consumption and an almost linear growth of average sizes of metal-containing nanoparticles with conversion. With the increase in constant k_1, the maximum rate increases, the induction period shortens, and the sizes of resulting particles decrease. After a certain period of growth, the number of particles reaches a limiting value which is lower than the greater the value of k_1 (**Figure 6**). At the same time, the mass of nanoparticles varies in proportion to conversion, irrespective of the constant (insert in **Figure 6**). At the same time, the narrow size distribution is typical of these particles.

Papers addressing methods of in situ obtainment of epoxy nanocomposites with metal nanoparticles are scarce.

Under UV radiation, 2,2'-dimethoxy-2-phenylacetophenone decomposes into radicals. A dimethoxyphenyl-carbonium radical reacts with $AgSbF_6$ and reduces a silver cation to Ag(0) via the transfer of electron, and then the radical transforms into the carbonium cation able to initiate the polymerization of diepoxide. Hence, silver nanoparticles and network matrix are formed simultaneously [121]. With increasing concentration of silver salt, the rate of polymerization and the ultimate conversion decrease, but the glass-transition temperature increases.

The silver nanoparticles with the same precursor, $AgSbF_6$, were obtained but in the presence of degradable under irradiation with visible light 3,5-bis(4-methoxyphenyl)-dithieno[3,2-b;2,3d]-thiophene [122]. A similar technique was employed to synthesize epoxy nanocomposites with nanoparticles of silver [123] and gold [124], but 2,3-bornadione (camphorquinone) was used as a source of radicals; in the case of gold, the precursor was $HAuCl_4$.

The silver nanoparticles in situ via the reduction of $AgNO_3$ in the epoxy resin by Triton-100, which simultaneously functioned as a stabilizer of nanoparticles, were
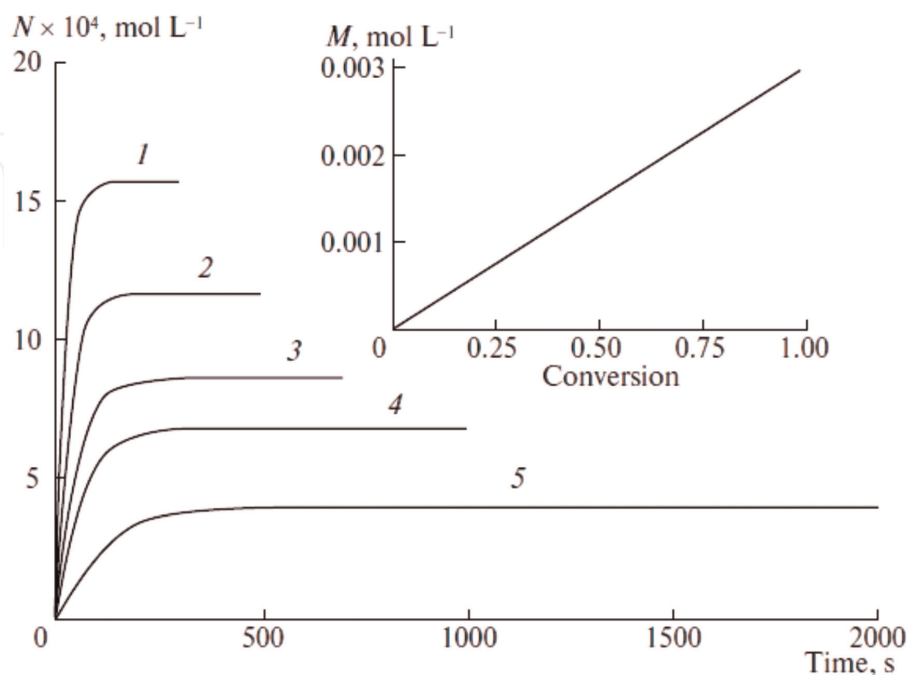

Figure 6.
Variation in N-value and mass M (insert) of nanoparticles; k_1, $L^2 \cdot mol^{-2} \cdot s^{-1}$ = (1) 10, (2) 30, (3) 50, (4) 100, and (5) 200. Reprinted with permission from IAPC "Nauka" [120].

synthesized [125]. A cycloaliphatic epoxy resin, hexahydro-4-methylphthalic anhydride as a curing agent, a reducing agent, and a precursor were dissolved in acetonitrile and exposed to UV radiation. After completion of the process, the solvent was removed at a reduced pressure.

A complex of silver acetate and 2-ethyl-4-methylimidazole was synthesized in an epoxy resin, and during its curing Ag^+ was reduced to $Ag(0)$ as a result of thermal decomposition of the complex [126]. In such a manner, silver nanoparticles were generated in situ. The imidazole product of complex decomposition served as a curing agent.

The epoxy resin ED-20 with triethylamine in the presence of silver myristate was cured [127–129]. The reduction of the latter and the formation of silver nanoparticles occurred simultaneously during polymerization. Reduction agents were both amine and the epoxy group. Carboxylate groups compatible with the medium functioned as stabilizers of particles.

4. Conclusion

It has been shown that, regardless of whether a filler is introduced in the reaction system or is formed in situ during the process of matrix formation, its structure changes to a greater or lesser extent than the unfilled cured epoxy binder. In addition, the matrix influences the character of distribution of nanoparticles over volume. This effect is especially important in the case of graphene and MMT, when exfoliation is the case in point. The matrix governs the size and shape of the resulting nanoparticles. They interact with the epoxy matrix through the resulting interfacial layers. There is no doubt that all these factors affect the properties of the epoxy nanocomposites.

The application areas of composites are defined by both the physicomechanical parameters of the epoxy matrix, its strength, thermomechanical stability, and adhesion ability and the unique properties of nanoparticles.

Nanoparticles of gold, silver, copper, TiO_2, ZnO, fullerene, and CNTs demonstrate effective antibacterial properties; therefore, composites containing these nanoparticles may be used for the microbiological control and purification of water, disinfection of surfaces, and creation of germicidal coatings, protective films, etc. Silver shows anti-inflammatory behavior and features antiviral and antifungal abilities. Its application in the form of nanoparticles (compared with the ionic form) decreases the cellular toxicity rather than the antibacterial efficiency [130].

Dielectric and magnetic epoxy nanocomposites have found wide use in such fields as Fourier spectroscopy, NMR, data storage, and absorption of electromagnetic radiation from other objects. The role of nanoparticles shows itself as improvement of electric strength and stress durability, suppression of space charge, and increase in the stability of dielectric discharge. For example, in the case of built-in planar capacitors, the insertion of dielectric films between copper sheets makes it possible to efficiently reduce the number of assembly devices. This not only leads to the miniaturization of circuit boards and electric wiring but also improves the characteristics of devices (e.g., promotes reduction in electromagnetic interference and switching noises) [131–133].

Epoxy resins are often employed in anti-wear applications. The use of such fillers as graphene oxide [134] or complexes MMT + SiO_2 [135], even at their very low content, decreases the rate of material wear by almost an order of magnitude.

The epoxy binders modified with carboxylated carbon nanotubes are more resistant to the action of aging factors. The presence of aggregates of carboxylated carbon nanotubes in the epoxy matrix positively influences the preservation of

physicomechanical properties of the composite subjected to heat and humidity aging. Microscopic examination revealed structural features of the epoxy nanocomposite and their effect on the resistance of the composite to the heat and humidity aging [136].

As for the use of epoxy nanocomposites in aerospace science and technology, this important problem, in author view, should be devoted to a special work. In short, it can be formulated as follows: structural nanocomposites, which are reinforcement structures based on carbon or glass fibers embedded in a polymer matrix modified with nanofillers, are the most important application of nanocomposites in the aerospace field [137], laminates, and sandwich structures. In addition, they can be used as anti-lightning [138], anti-radar [139] protection devices, flame retardant, and heat-resistant paints [140], ameliorating anti-corrosion performances [141].

Author details

Vadim Irzhak
Institute of Problems of Chemical Physics Russian Academy of Sciences, Chernogolovka, Moscow Region, Russian Federation

*Address all correspondence to: irzhak@icp.ac.ru

IntechOpen

References

[1] Ramdani N. editor. Nanotechnology in Aerospace and Structural Mechanics. Hershey PA: IGI Global; 2019

[2] Irzhak TF, Irzhak VI. Epoxy nanocomposites. Polymer Sciences, A. 2017;**59**(6):791-825

[3] Lee H, Neville K. Handbook of Epoxy Resins. New York: McGraw-Hill; 1967

[4] Chernin IZ, Smekhov FM, Zherdev YV. Epoxy Polymers and Compositions. Moscow: Khimiya; 1982. [in Russian]

[5] Khozin VG. Reinforcement of Epoxy Polymers. Kazan: Dom Pechati; 2004. [in Russian]

[6] Irzhak VI, Rozenberg BA, Enikolopyan NS. Network Polymers: Synthesis, Structure, Properties. Moscow: Nauka; 1979. [in Russian]

[7] Rozenberg BA. Kinetics, thermodynamics and mechanism of reactions of epoxy oligomers with amines. Advances in Polymer Science. 1986;**75**:113-165

[8] Okabe T, Takehara T, Inose K, Hirano N, Nishikawa M, Uehara T. Curing reaction of epoxy resin composed of mixed base resin and curing agent: Experiments and molecular simulation. Polymer. 2013; **54**(17):4660-4668

[9] Irzhak VI. Epoxide composite materials with carbon nanotubes. Russian Chemical Reviews. 2011;**80**(8): 787-806

[10] Kablov EN, Kondrashov SV, Yurkov GY. Prospects of using carbonaceous nanoparticles in binders for polymer composites. Nanotechnologies in Russia. 2013;**8**(3-4):163-185

[11] Song SH, Park KH, Kim BH, Choi YW, Jun GH, Lee DJ, et al. Enhanced thermal conductivity of epoxy/graphene composites by using non-oxidized graphene flakes with non-covalent functionalization. Advances in Materials. 2013;**25**(5):732-737

[12] Vyazovkin S, Sbirrzaauoli N. Mechanism and kinetics of epoxy-amine cure studied by differential scanning calorimetry. Macromolecules. 1996; **29**(6):1867-1873

[13] D'yachkov PN. Carbon Nanotubes: Structure, Properties, Application. Moscow: Binom; 2006. [in Russian]

[14] Grayfer ED, Makotchenko VG, Nazarov AS, Kim SJ, Fedorov VE. Graphene: Chemical approaches to the synthesis and modification. Russian Chemical Reviews. 2011;**80**(8):751-704

[15] Ivanovskii AL. Graphene-based and graphene-like materials. Russian Chemical Reviews. 2012;**81**(7):571-605

[16] Rakov EG. Nanotubes and Fullerenes. Moscow: Universitetskaya Kniga; 2006. [in Russian]

[17] Rakov EG. Carbon nanotubes in new materials. Russian Chemical Reviews. 2013;**82**(1):27-47

[18] Schaetz A, Zeltner M, Stark WJ. Carbon modifications and surfaces for catalytic organic transformations. ACS Catalysis. 2012;**2**(6):1267-1284

[19] Navalon S, Dhakshinamoorthy A, Alvaro M, Garcia H. Carbocatalysis by graphene-based materials. Chemical Reviews. 2014;**114**(12):6179-6212

[20] Chua CK, Pumera M. Carbocatalysis: The state of "Metal-Free" catalysis. Chemistry–A European Journal. 2015;**21**(36):12550-12562

[21] Liang Z, Gou J, Zhang C, Wang B, Kramer L. Investigation of molecular

interactions between (10, 10) single-walled nanotube and epon 862 resin/DETDA curing agent molecules. Materials Science and Engineering A. 2004;**365**(1–2):228-234

[22] Britz DA, Khlobystov AN. Noncovalent interactions of molecules with single walled carbon nanotubes. Chemical Society Reviews. 2006;**35**(7): 637-659

[23] Shen B, Zhai W, Tao M, Lu D, Zheng W. Enhanced interfacial interaction between polycarbonate and thermally reduced graphene induced by melt blending. Composites Science and Technology. 2013;**77**:87-110

[24] Xue B, Zhu J, Liu N, Li Y. Facile functionalization of graphene oxide with ethylenediamine as a solid base catalyst for knoevenagel condensation reaction. Catalysis Communications. 2015;**64**:105-109

[25] Xie H, Liu B, Yuan Z, Shen J, Cheng R. Cure kinetics of carbon nanotube/tetrafunctional epoxy nanocomposites by isothermal differential scanning calorimeter. Journal of Polymer Science, Part A: Polymer Chemistry. 2004;**42**(20):3701-3712

[26] Tao K, Yang S, Grunlan JC, Kim YS, Dang B, Deng Y, et al. Effects of Carbon Nanotube Fillers on the Curing Processes of Epoxy Resin-Based Composites. Journal of Applied Polymer Science. 2006;**102**(6):5248-5254

[27] Esmizadeh E, Yousefi A, Naderi G. Effect of type and aspect ratio of different carbon nanotubes on cure behavior of epoxy-based nanocomposite. Iranian Polymer Journal. 2015;**24**(1):1-12

[28] Visco A, Calabrese L, Milone C. Cure rate and mechanical properties of a DGEBF epoxy resin modified with carbon nanotubes. Journal of Reinforced Plastics and Composites. 2009;**28**(8): 937-949

[29] Susin SB, Pistor V, Amico SC, Coelho LAF, Pezzin SH, Zattera AJ. Investigation of cure kinetics in epoxy/multi-walled carbon nanotube nanocomposites. Journal of Applied Polymer Science. 2014;**131**(3): 39857-39862

[30] Rahaman A, Mohanty A. Effect of carbon nanotubes on the curing and thermomechanical behavior of epoxy/carbon nanotubes composites. Polymer Composites. 2014;**35**(29):441-449

[31] Cividanes LS, Simonetti EA, Moraes MB, Fernandes FW, Thim GP. Influence of carbon nanotubes on epoxy resin cure reaction using different techniques: A comprehensive review. Polymer Engineering and Science. 2014;**54**(11): 2461-2469

[32] Zhou T, Wang X, Wang T. Cure reaction of multi-walled carbon nanotubes/diglycidyl ether of bisphenol A/2-ethyl-4-methylimidazole (MWCNTs/DGEBA/EMI-2,4) nanocomposites: Effect of carboxylic functionalization of WCNTs. Polymer International. 2009;**58**(4):445-452

[33] Abdalla M, Dean D, Robinson P, Nyairo E. Cure behavior of epoxy/MWCNT nanocomposites: The effect of nanotube surface modification. Polymer. 2008;**49**(16):3310-3317

[34] Valentini L, Puglia D, Carniato F, Boccaleri E, Marchese L, Kenny JM. Use of plasma fluorinated single-walled carbon nanotubes for the preparation of nanocomposites with epoxy matrix. Composites Science and Technology. 2008;**68**(3–4):1008-1014

[35] Qiu J, Wang S. Reaction kinetics of functionalized carbon nanotubes reinforced polymer composites. Materials Chemistry and Physics. 2010; **121**(1–2):295-301

[36] Choi WJ, Powell RL, Kim DS. Curing behavior and properties of epoxy nanocomposites with amine functionalized multiwall carbon nanotubes. Polymer Composites. 2009;**30**(4):415-421

[37] Yang K, Gu M, Jin Y, Mu G, Pan X. Influence of surface treated multi-walled carbon nanotubes on cure behavior of epoxy nanocomposites. Composites Part A Applied Science and Manufacturing. 2008;**39**(10):1670-1678

[38] Cividanes LS, Brunelli DD, Antunes EF, Corat EJ, Sakane KK, Thim GP. Cure study of epoxy resin reinforced with multiwalled carbon nanotubes by raman and luminescence spectroscopy. Journal of Applied Polymer Science. 2013;**127**(1):544-553

[39] Grachev VP, Kondrashov SV, Akatenkov RV, Aleksashin VN, Deev IS, Anoshkin IV, et al. Modification of epoxy polymers by small additives of multiwall carbon nanotube. Polymer Science, Series A. 2014;**56**(3):330-336

[40] Qiu SL, Wang CS, Wang YT, Liu CG, Chen XY, Xie HF, et al. Reaction kinetics of functionalized carbon nanotubes reinforced polymer composites. eXPRESS Polymer Letter. 2011;**5**(9):809-818

[41] Ryu SH, Sin JH, Shanmugharaj AM. Study on the effect of hexamethylene diamine functionalized graphene oxide on the curing kinetics of epoxy nanocomposites. European Polymer Journal. 2014;**52**:88-97

[42] Park JK, Kim DS. Effects of an aminosilane and a tetra-functional epoxy on the physical properties of di-functional epoxy/graphene nanoplatelets nanocomposites. Polymer Engineering and Science. 2014;**54**(4): 969-976

[43] Park JK, Kim DS. Preparation and physical properties of an epoxy nanocomposite with amine-functionalized graphenes. Polymer Engineering and Science. 2014;**54**(5): 985-991

[44] Galpaya DGD, Fernando JFS, Rintoul L, Motta N, Waclawik ER, Yan C, et al. The effect of graphene oxide and its oxidized debris on the cure chemistry and interphase structure of epoxy nanocomposites. Polymer. 2015;**71**:122-134

[45] Acocella MR, Corcione CE, Giuri A, Maggio M, Maffezzoli A, Guerra G. Graphene oxide as a catalyst for ring opening reactions in amine crosslinking of epoxy resins. RSC Advances. 2016;**6**(28):23858-23866

[46] Mauro M, Acocella MR, Corcione CE, Maffezzoli A, Guerra G. Catalytic activity of graphite-based nanofillers on cure reaction of epoxy resins. Polymer. 2014;**55**:5612-5615

[47] Li L, Zeng Z, Zou H, Liang M. Curing characteristics of an epoxy resin in the presence of functional graphite oxide with amine-rich surface. Thermochimica Acta. 2015;**614**:76-102

[48] Seyhan AT, Sun Z, Deitzel J, Tanoglu M, Heider D. Cure kinetics of vapor grown carbon nanofiber (VGCNF) modified epoxy resin suspensions and fracture toughness of their resulting nanocomposites. Materials Chemistry and Physics. 2009;**118**(1):234-242

[49] Cai ZQ, Movva S, Chiou NR, Guerra D, Hioe Y, Castro JM, et al. Effect of polyaniline surface modification of carbon nanofibers on cure kinetics of epoxy resin. Journal of Applied Polymer Science. 2010;**118**(4):2328-2335

[50] Sanctuary R, Baller J, Zielinski B, Becker N, Krüger K, Philipp U, et al. Influence of Al_2O_3 nanoparticles on the isothermal cure of an epoxy resin.

Journal of Physics: Condensed Matter. 2009;**21**(3):035118-035126

[51] Balle J, Becker N, Ziehmer M, Thomassey M, Zielinski B, Müller U, et al. Interactions between silica nanoparticles and an epoxy resin before and during network formation. Polymer. 2009;**50**(14):3211

[52] Karasinski EN, Da Luz MG, Lepienski CM, Coelho LAF. Nanostructured coating based on epoxy/metal oxides: Kinetic curing and mechanical properties. Thermochimica Acta. 2013;**569**:167-211

[53] Zabihi O, Mostafavi SM, Ravari F, Khodabandeh A, Hooshafza A, Zare K, et al. The effect of zinc oxide nanoparticles on thermo-physical properties of diglycidyl ether of bisphenol A/2,2-diamino-1,1-binaphthalene nanocomposites of surface treated multi-walled carbon nanotubes on cure behavior of epoxy nanocomposite. Thermochimica Acta. 2011;**521**(1–2):49-58

[54] Ghaffari M, Ehsani M, Vandalvand M, Avazverdi E, Askari A, Goudarzi A. Studying the effect of micro- and nano-sized ZnO particles on the curing kinetic of epoxy/polyaminoamide system. Progress in Organic Coatings. 2015;**89**: 277-283

[55] Zabihi O, Hooshafza A, Moztarzadeh F, Payravand H, Afshar A, Alizadeh R. Isothermal curing behavior and thermo-physical properties of epoxy-based thermoset nanocomposites reinforced with Fe_2O_3 nanoparticles. Thermochimica Acta. 2012;**527**:190-198

[56] Omrani A, Rostami AA, Ravari F, Mashak A. Curing behavior and structure of a novel nanocomposite from glycerol diglycidyl ether and 3,3-dimethylglutaric anhydride. Thermochimica Acta. 2011;**517**(1–2): 9-15

[57] Hong SG, Tsai JS. The adsorption and curing behavior of the epoxy/amidoamine system in the presence of metal oxides. Journal of Thermal Analysis and Calorimetry. 2001;**63**(1): 31-46

[58] Baller J, Thomassey M, Ziehmer M, Sanctuary R. The catalytic influence of alumina nanoparticles on epoxy curing. Thermochimica Acta. 2011;**517**(1–2): 34-39

[59] Ghaemy M, Amini Nasab SM, Barghamadi M. Nonisothermal cure kinetics of diglycidylether of bisphenol-A/amine system reinforced with nanosilica particles. Journal of Applied Polymer Science. 2007;**104**(6): 3855-3863

[60] Rosso P, Ye L. Epoxy/silica nanocomposites: Nanoparticle-induced cure kinetics and microstructure. Macromolecular Rapid Communications. 2007;**28**(1):121-126

[61] Alzina C, Sbirrazzuoli N, Mija A. Epoxy-amine based nanocomposites reinforced by silica nanoparticles. Relationships between morphologic aspects, cure kinetics, and thermal properties. Journal of Physical Chemistry C. 2011;**115**(46):22789-22795

[62] Pavlidou S, Papaspyrides CD. A review on polymer–layered silicate nanocomposites. Progress in Polymer Science. 2008;**33**(12):1119-1198

[63] Becker O, Simon PG. Epoxy layered silicate nanocomposites. Advances in Polymer Science. 2005;**179**:29-82

[64] Paiva LB, de Morales AR, Valenzuela Diaz FR. Organoclays: Properties, preparation and application. Applied Clay Science. 2008;**42**(1–2): 8-24

[65] Alzina C, Mija A, Vincent L, Sbirrazzuoli N. Effects of incorporation of organically modified montmorillonite

on the reaction mechanism of epoxy/amine cure. The Journal of Physical Chemistry. B. 2012;**116**(19):5786-5794

[66] Ivankovic M, Brnardic I, Ivankovic H, Mencer HJ. DSC study of the cure kinetics during nanocomposite formation: Epoxy/poly(oxypropylene) diamine/organically modified montmorillonite system. Journal of Applied Polymer Science. 2006;**99**(2): 550-557

[67] Román F, Calventus Y, Colomer P, Hutchinson JM. Effect of carbon nanotubes on the curing and thermomechanical behavior of epoxy/carbon nanotubes composites. Thermochimica Acta. 2012;**541**:76-85

[68] Alzina C, Sbirrazzuoli N, Mija A. Hybrid Nanocomposites: Advanced nonlinear method for calculating key kinetic parameters of complex cure kinetics. The Journal of Physical Chemistry. B. 2010;**114**(39): 12480-12487

[69] Li L, Zou H, Liang M, Chen Y. Study on the effect of poly(oxypropylene) diamine modified organic montmorillonite on curing kinetics of epoxy nanocomposites. Thermochimica Acta. 2014;**597**:93-100

[70] Ferdosian F, Ebrahimi M, Jannesari A. Curing kinetics of solid epoxy/DDM/nanoclay: Isoconversional models versus fitting model. Thermochimica Acta. 2013;**568**:67-73

[71] Shanmugharaj AM, Ryu SH. Study on the effect of aminosilane functionalized nanoclay on the curing kinetics of epoxy nanocomposites. Thermochimica Acta. 2012;**546**:16-23

[72] Shiravand F, Hutchinson JM, Calventus Y. Influence of the isothermal cure temperature on the nanostructure and thermal properties of an epoxy layered silicate nanocomposite. Polymer Engineering and Science. 2014;**54**(1):51-58

[73] Montserrat S, Román FM, Hutchinson J, Campos L. Analysis of the cure of epoxy based layered silicate nanocomposites: Reaction kinetics and nanostructure development. Journal of Applied Polymer Science. 2008;**108**(2):923-938

[74] Cortés P, Fraga I, Calventus Y, Román F, Hutchinson JM, Ferrando F. A new epoxy-based layered silicate nanocomposite using a hyperbranched polymer: Study of the curing reaction and nanostructure development. Materials. 2014;**7**(3):1830-1849

[75] Shiravand F, Fraga I, Cortés P, Calventus Y, Hutchinson JM. Thermal analysis of polymer layered silicate nanocomposites: Identification of nanostructure development by DSC. Journal of Thermal Analysis and Calorimetry. 2014;**118**(2):723-729

[76] Shiravand F, Hutchinson JM, Calventus Y. Non-isothermal cure and exfoliation of tri-functional epoxy-clay nanocomposites. Express Polymer Letters. 2015;**9**(8):695-708

[77] Kong D, Park CE. Real time exfoliation behavior of clay layers in epoxy-clay nanocomposites real time exfoliation behavior of clay layers in epoxy-clay nanocomposites. Chemistry of Materials. 2003;**15**(2):419-424

[78] Hutchinson JM, Shiravand F, Calventus Y. Intra- and extra-gallery reactions in tri-functional epoxy polymer layered silicate nanocomposites. Journal of Applied Polymer Science. 2013;**128**(5):2961-2970

[79] Pustkova P, Hutchinson JM, Román F, Montserrat S. Homopolymerization effects in polymer layered silicate nanocomposites based upon epoxy resin: Implications for exfoliation. Journal of Applied Polymer Science. 2009;**114**(2):1040-1447

[80] Hutchinson JM, Shiravand F, Calventus Y, Fernández-Francos X,

Ramis X. Highly exfoliated nanostructure in trifuncional epoxy/clay nanocomposites using boron trifluoride as initiator. Journal of Applied Polymer Science. 2014;**131**(6): 40020-40029

[81] Jagtap SB, Rao VS, Barman S, Ratna D. Nanocomposites based on epoxy resin and organoclay functionalized with a reactive modifier having structural similarity with the curing agent. Polymer. 2015;**63**:41-71

[82] Pomogailo AD, Rozenberg AS, Dzhardimalieva GI. Metal-Polymer Nanocomposites. Hoboken: Wiley; 2005

[83] Wilcoxon JP, Abrams BL. Synthesis, structure and properties of metal nanoclusters. Chemical Society Reviews. 2006;**35**(4):1162-1194

[84] Gusev AI. Nanomaterials, Nanostructures, Nanotechnologies. Moscow: Fizmatlit; 2007. [in Russian]

[85] Suzdalev IP. Nanotechnology: Physics and Chemistry of Nanocrystals, Nanostructures and Nanomaterials. Moscow: Kom Kniga; 2006. [in Russian]

[86] Faraji M, Yamini Y, Rezaee M. Magnetic nanoparticles: Synthesis, stabilization, functionalization, characterization, and applications. Journal of the Iranian Chemical Society. 2010;**7**(1):1-37

[87] Lu Y, Chen W. Sub-nanometre sized metal clusters: From synthetic challenges to the unique property discoveries. Chemical Society Reviews. 2012;**41**(9):3594-3624

[88] Agareva NA, Aleksandrov AP, Smirnova LA, Bityurin NM. Synthesis of block polymethylmethacrylate containing precursor for photoinduced formation of gold nanoparticles. Perspektivnye Materialy. 2009;**1**:5-12

[89] Rozenberg BA, Tenne R. Polymer-assisted fabrication of nanoparticles and nanocomposites. Progress in Polymer Science. 2008;**33**(1):40-112

[90] Wuithschick M, Paul B, Bienert R, Sarfraz A, Vainio U, Sztucki M, et al. Size-controlled synthesis of colloidal silver nanoparticles based on mechanistic understanding. Chemistry of Materials. 2013;**25**(24):4679-4689

[91] Wang F, Richards VN, Shields SP, Buhro WE. Kinetics and mechanisms of aggregative nanocrystal growth. Chemistry of Materials. 2014;**26**(1):5-21

[92] Yan S, Wu Z, Yu H, Gong Y, Tan Y, Du R, et al. Time-resolved small-angle X-ray scattering study on the growth behavior of silver nanoparticles. The Journal of Physical Chemistry. 2014; **118**(21):11454-11463

[93] Völkle CM, Gebauer D, Cölfen H. High-resolution insights into the early stages of silver nucleation and growth. Faraday Discussions. 2015;**179**:59-69

[94] Irzhak VI. The mechanisms of the formation of metal-containing nanoparticles. Review Journal of Chemistry. 2016;**6**(4):370-404

[95] Volmer M. Kinetik der Phasenbildung. Dresden: Steinkopff; 1939

[96] Frenkel' YI. Kineticheskaya Teoriya Zhidkostei (Kinetic Theory of Liquids). Leningrad: Nauka; 1975

[97] LaMer VK, Dinegar RH. Theory, production and mechanism of formation of monodispersed hydrosols. Journal of the American Chemical Society. 1950;**72**(11):4847-4854

[98] Polte J, Tuaev X, Wuithschick M, Fischer A, Thuenemann AF, Rademann K, et al. Formation mechanism of colloidal silver nanoparticles: Analogies and differences to the growth of gold

nanoparticles. ACS Nano. 2012;**6**(7): 5791-5802

[99] Turkevich J, Stevenson PC, Hillier J. A study of the nucleation and growth processes in the synthesis of colloidal gold. Faraday Discussions of the Chemical Society. 1951;**11**:55-75

[100] Finney EE, Finke RG. Nanocluster nucleation and growth kinetic and mechanistic studies: A review emphasizing transition-metal nanoclusters. Journal of Colloid and Interface Science. 2008;**317**(2):351-374

[101] Watzky MA, Finke RG. Nanocluster size-control and "Magic Number" investigations. Experimental tests of the "Living-Metal Polymer" concept and of mechanism-based size-control reductions leading to the syntheses of Ir(0) nanoclusters centering about four sequential magic numbers. Chemistry of Materials. 1997; **9**(12):3083-3095

[102] Bogdanova LM, Shershnev VA, Spirin MG, Irzhak VI, Dzhardimalieva GI. Evolution of silver nanoparticles synthesized in situ in a polycondensation epoxy matrix. Russian Journal of Physical Chemistry A. 2019; **93**(7):1043-1047

[103] Irzhak VI. Digestive ripening of nanoparticles. Russian Journal of Physical Chemistry A. 2017;**91**(8): 1502-1506

[104] Lifshits M, Slezov VV. Kinetics of diffusive decomposition of supersaturated solid solutions. Journal of Experimental and Theoretical Physics. 1959;**35**(2):479-492

[105] Wagner Z. Theorie der alterung von niderschlagen durch umlösen (ostwald reifung). Zeitschrift für Elektrochemie. 1961;**65**:581-591

[106] Xin HLL, Zheng HM. In situ observation of oscillatory growth of

bismuth nanoparticles. Nano Letters. 2012;**12**(3):1470-1474

[107] Bardaji M, Uznanski P, Amiens C, Chaudret B, Laguna A. Aurophilic complexes as gold atom sources in organic media. Chemical Communications. 2002;**6**:598-599

[108] Nakamoto M, Kashiwagi Y, Yamamoto M. Synthesis and size regulation of gold nanoparticles by controlled thermolysis of ammonium gold(I) thiolate in the absence or presence of amines. Inorganica Chimica Acta. 2005;**358**(14):4229-4236

[109] Gur'eva LL, Tkachuk AI, Kuzub LI, Estrina GA, Knerel'man EI, Khodos II, et al. Synthesis of silver nanoparticles with polystyrylcarboxylate ligands. Journal of Polymer Science, Series B. 2013;**55**(3–4):139-146

[110] Kuzub LI, Gur'eva LL, Grishchuk AA, Estrina GA, Estrin YI, Badamshina ER. Regularities of the formation of silver nanoparticles with oligostyrylcarboxylate ligands. Journal of Polymer Science, Series B. 2015;**57**(6): 608-615

[111] Kuzub LI, Gur'eva LL, Khodos II, Grishchuk AA, Estrin YI, Badamshina ER. Regularities of the formation of silver nanoparticles with oligostyrylmonocarboxylate ligands in ED-20 oligomer. Journal of Polymer Science, Series B. 2017;**59**(5):537-543

[112] Yamamoto M, Nakamoto M. Novel preparation of monodispersed silver nanoparticles via amine adducts derived from insoluble silver myristate in tertiary alkylamine. Journal of Materials Chemistry. 2003;**13**(9):2064-2065

[113] Yamamoto M, Kashiwagi Y, Nakamoto M. Size-controlled synthesis of monodispersed silver nanoparticles capped by long-chain alkyl carboxylates from silver carboxylate and tertiary

amine. Langmuir. 2006;**22**(20): 8581-8586

[114] Kashiwagi Y, Yamamoto M, Nakamoto M. Facile size-regulated synthesis of silver nanoparticles by controlled thermolysis of silver alkylcarboxylates in the presence of alkylamines with different chain lengths. Journal of Colloid and Interface Science. 2006;**300**(1):169-175

[115] Khanna PK, Kulkarni D, Beri RK. Synthesis and characterization of myristic acid capped silver nanoparticles. Journal of Nanoparticle Research. 2008;**10**(6):1059-1062

[116] Clary DR, Mills G. Photochemical generation of nanometer-sized Cu particles in octane. The Journal of Physical Chemistry, C. 2011;**115**(30): 14656-14663

[117] Clary DR, Nabil M, Sedeh MM, El-Hasadi Y, Mills G. Photochemical generation of Ag, Pd, and Pt particles in octane. The Journal of Physical Chemistry, C. 2012;**116**(16):9243-9250

[118] Kuzub LI, Bogdanova LM, Kurkin TS, Torbov VI, Gur'eva LL, Rozenberg BA, et al. Investigation of the Regularities of Synthesis of Monodisperse Silver Nanoparticles with Chemically Bound Organic Ligands: Proceeding of Articles "Structure and Dynamics of Molecular Systems", 2009, Yal'chik, Russia. Ioshkar-Ola: MarGTU; 2009. Part 2, No 16, pp. 134-139

[119] Kuzub LI, Bogdanova LM, Kurkin TS, Buzin PV. Principal Aspects of the Synthesis of Silver Nanoparticles with Carboxylate Ligands: Proceeding of Articles "Structure and Dynamics of Molecular Systems", 2010, Yal'chik, Russia. Ioshkar-Ola: MarGTU; 2010. Part 1, No 17. pp. 340-345

[120] Solov'ev ME, Irzhak TF, Irzhak VI. Kinetics of formation of nanoparticles from first group metal carboxylates.

Russian Journal of Physical Chemistry A. 2015;**89**(3):1642-1647

[121] Sangermano M, Yagci Y, Rizza G. In situ synthesis of silver-epoxy nanocomposites by photoinduced electron transfer and cationic polymerization processes. Macromolecules. 2007;**40**(25): 8827-8829

[122] Yagci Y, Sahin O, Ozturk T, Marchi S, Grassini S, Sangermano M. Synthesis of silver/epoxy nanocomposites by visible light sensitization using highly conjugated thiophene derivatives. Reactive and Functional Polymers. 2011; **71**(7):857-862

[123] Yagci Y, Sangermano M, Rizza GA. Visible light photochemical route to silver–epoxy nanocomposites by simultaneous polymerization–Reduction approach. Polymer. 2008; **49**(24):5195-5198

[124] Yagci Y, Sangermano M, Rizza G. Synthesis and characterization of gold-epoxy nanocomposites by visible light photoinduced electron transfer and cationic polymerization processes. Macromolecules. 2008;**41**(20): 7268-7270

[125] Lu J, Moon KS, Wong CP. Silver/ polymer nanocomposite as a high-*k* polymer matrix for dielectric composites with improved dielectric performance. Journal of Materials Chemistry. 2008;**18**(40):4821-4826

[126] Gao H, Liu L, Luo Y, Jia D. In-situ preparation of epoxy/silver nanocomposites by thermal decomposition of silver–imidazole complex. Materials Letters. 2011;**65** (23–24):3529-3532

[127] Bogdanova L, Kuzub L, Dzhavadjan E, Rabenok E, Novikov G, Pomogailo A. In situ synthesis and properties of epoxy nanocomposites.

Macromolecular Symposia. 2012;
317–318:117-122

[128] Bogdanova LM, Kuzub LI, Dzhavadyan EA, Torbov VI, Dremova NN, Pomogailo AD. Mechanical properties of epoxy composites based on silver nanoparticles formed in situ. Journal of Polymer Science, Series A. 2014;**56**(3):304-310

[129] Bogdanova LM, Kuzub LI, Spirin MG, Dzhardimalieva GI, Irzhak VI. Features of the synthesis of silver nanoparticles in a curing epoxy matrix. Vestnik KGTU. 2015;**18**(16):10-15

[130] Gu H, Tadakamalla S, Huang Y, Colorado HA, Luo Z, Haldolaarachchige N, et al. Polyaniline stabilized magnetite nanoparticle reinforced epoxy nanocomposites. ACS Applied Materials & Interfaces. 2012;**4**(10):5613-5624

[131] Huang X, Xie L, Yang K, Wu C, Jiang P, Li S, et al. Role of interface in highly filled epoxy/BaTiO$_3$ nanocomposites. Part I-correlation between nanoparticle surface chemistry and nanocomposite dielectric property. IEEE Transactions on Dielectrics and Electrical Insulation. 2014;**21**(2):467-479

[132] Novikov GF, Rabenok EV, Bogdanova LM, Irzhak VI. Temperature dependence of direct current conductivity in Ag-ED20 nanocomposite films. Russian Journal of Physical Chemistry A. 2017;**91**(10):1971-1975

[133] Novikov GF, Rabenok EV, Bogdanova LM, Irzhak VI. Dielectric properties of films of Ag-ED20 epoxy nanocomposite synthesized in situ. Temperature dependence of direct current conductivity. Journal of Polymer Science: Part A. 2017;**59**(5):741-750

[134] Shen XJ, Pei XQ, Fu SY, Friedrich K. Significantly modified tribological performance of epoxy nanocomposites at very low graphene oxide content. Polymer. 2013;**54**(3):1234-1242

[135] Thind KS, Singh J, Saini JS, Bhunia H. Mechanical and wear properties of hybrid epoxy nanocomposites. Indian Journal of Engineering and Materials Science. 2015;**22**(4):421-428

[136] Kondrashov SV, Merkulova YI, Marakhovskii PS, D'yachkova TP, Shashkeev KA, Popkov OV, et al. Degradation of physicomechanical properties of epoxy nanocomposites with carbon nanotubes upon heat and humidity aging. Russian Journal of Applied Chemistry. 2017;**90**(5):788-796

[137] Dinca I, Ban C, Stefan A, Pelin G. Nanocomposites as advanced materials for aerospace industry. INCAS Bulletin. 2012;**4**(4):73-83

[138] Katunin A, Krukiewicz K, Turczyn R, Sul P, Łasica A, Bilewicz M. Synthesis and characterization of the electrically conductive polymeric composite for lightning strike protection of aircraft structures. Composite Structures. 2017;**159**:773-783

[139] Govindaraj B, Sarojadevi M. Microwave-assisted synthesis of nanocomposites from polyimides chemically cross-linked with functionalized carbon nanotubes for aerospace applications. Polymers for Advanced Technologies. 2018;**29**(6):1718-1726

[140] Meenakshi KS, Sudhan EPJ. Development of novel TGDDM epoxy nanocomposites for aerospace and high performance applications—Study of their thermal and electrical behavior. Arabian Journal of Chemistry. 2016;**9**(1):79-85

[141] Monetta T, Acquesta A, Bellucci F. Graphene/epoxy coating as multifunctional material for aircraft structures. Aerospace. 2015;**2**(3):423-434